

Factorization of the t -channel pole in quark-gluon scatteringJeppe R. Andersen¹ and Jennifer M. Smillie²¹*Theory Division, Physics Department, CERN, CH-1211 Geneva 23, Switzerland*²*Department of Physics and Astronomy, UCL, Gower Street, London, United Kingdom WC1E 6BT*

(Received 15 April 2010; published 11 June 2010)

By exploring specific helicity states in quark-gluon scattering at tree level we show explicitly that the full t -channel pole can be described exactly as a contraction of two local currents. In the four cases of helicity assignment where a channel exists also for qQ -scattering, qg -scattering is described exactly by this t -channel pole. Only in two of the four remaining helicity assignments is there a contribution from u - and s -channel poles. We extract a gauge-invariant definition for the t -channel current generated by the scattering of a gluon and offer an interpretation of the form.

DOI: 10.1103/PhysRevD.81.114021

PACS numbers: 13.85.Hd

I. INTRODUCTION

At the LHC, most studies of physics from both within and possibly beyond the standard model will require a detailed understanding of not just the rate but also the topology of hard multijet events. The vast phase space opened by the center-of-mass energy of the accelerator can counteract the α_s -suppression of further radiation in the hard-scattering matrix element.¹

This means that it is not only relevant to calculate processes of ever higher multiplicity at the lowest order in perturbation theory, but the description of even *hard* radiative corrections to these tree-level configurations becomes increasingly relevant. To date, the radiative corrections for LHC processes with two or more QCD charged particles in the final state are known in full fixed order perturbation theory only to the first order (i.e. the process is known to next-to-leading order). Radiative corrections beyond the first order have traditionally been approximated within a parton shower approach [1–3]. The approximations applied to the real emissions become exact in the soft and collinear limits, and result in a sufficiently simple formalism that all-order results can be obtained. Virtual corrections are defined by keeping the shower evolution unitary (i.e. the probability for emitting or not emitting equal to one; in the language of fixed order calculations, the K -factor induced by the parton shower for the inclusive cross section is one).

The perturbative corrections simplify not just in the soft and collinear limit, but also in the limit of large invariant mass between all produced particles, the limit of so-called *multi-Regge kinematics* (MRK), where the all-order per-

turbative results for $2 \rightarrow n$ -scattering are known not just for the real but also virtual corrections [4–6]. This limit is of interest when the focus is on describing correctly the number and topology of jets (rather than the radiation within each jet), since any jet definition introduces a requirement of a non-negligible invariant mass between the constituents of separate jets.

We have recently presented a framework[7], which not only reproduces the exact $2 \rightarrow n$ results in the MRK limit, but also reproduces to a good degree the results obtained using full perturbative QCD order-by-order (for the low orders where such results can be obtained) for completely inclusive calculations, i.e. without special cuts in phase space. The amplitude for the scattering is described by a basic $2 \rightarrow 2$ -scattering under the exchange of the current generated by the deflection of each particle, supplemented by effective vertices for the extra gluon emission. These effective vertices take into account the emission off each of the four legs of the basic (or backbone) $2 \rightarrow 2$ process, and emission off the exchanged current. The formulation of Ref. [7] in terms of current scattering of specific helicity states provides the crucial improvement over initial efforts in Ref. [8,9], and extends the phase space region of applicability even further. The point of constructing the approximations to the perturbative series is to obtain a formalism which is sufficiently simple to allow for the all-order sum to be constructed directly, while being sufficiently accurate when compared order-by-order to the full fixed-order results where these can be obtained. The approximating all-order sum can be matched to the tree-level n -jet rates, where these are known. See Ref. [7] and Appendix B for further details.

In the MRK limit, the kinematical dependence of the amplitude for quark-quark, quark-gluon, and gluon-gluon scattering is identical, and the scattering amplitude differs only by color factors. In this limit, the scattering amplitude is dominated by the behavior dictated by the poles in the t -channel momenta. Therefore, the picture advocated in Ref. [7] is built on the basic structure of the scattering of

¹This is true, in particular, for processes where the partonic cross section is not suppressed with increasing partonic center-of-mass energy \hat{s} , such as e.g. $2 \rightarrow 2$ processes which can proceed through a t -channel exchange of a gluon. For large \hat{s} the partonic cross section for such processes limits to a constant depending on the transverse momentum only. All other $2 \rightarrow 2$ processes are suppressed by powers of \hat{s} .

two different quark flavors $qQ \rightarrow qQ$, which at lowest order proceeds through the exchange of a single gluon in the t -channel. The results for gluon scattering are found by using the same color factor replacement $C_F \rightarrow C_A$ that arises in the *effective PDF approach* [10].

The description of the basic $2 \rightarrow 2$ -scattering is therefore one of the contraction of two generated currents, each of the form $A^\mu = \bar{\psi} \gamma^\mu \psi$. We will call this form of the matrix element “ t -channel factorized,” because each current obviously depends on the momenta of the local scattering spinors only, and the amplitude has a pole only in the t -channel. As already mentioned, the factorized form arising for the scattering of quarks was used also for gluon scattering in Ref. [7], changing only the effective color factor. This results in the right MRK limit also for processes with gluon scattering.

A priori, one might worry about extending the simple description in quark-quark scattering to processes involving gluons, since e.g. there are three Feynman diagrams contributing to $qg \rightarrow qg$ instead of the one in $qQ \rightarrow qQ$, with apparent singularities in the s - and u -channels (see Fig. 1). In Sec. II we will show explicitly that the full tree-level scattering for $qg \rightarrow qg$ factorizes completely according to the above definition for all except two (suppressed) out of eight nonequivalent helicity configurations. In fact, for the helicity assignments where a channel exists also for qQ -scattering, the square of the matrix element for qg -scattering is equal to that of qQ -scattering, times a factor depending only on the light-cone momenta of the gluons. And even in the four remaining kinematically suppressed channels, the t -channel singularity is completely factorized. We thereby obtain a gauge-invariant definition of the off-shell current generated by the scattering of a gluon, by using the natural definition of the current as the full coefficient of the t -channel pole.

While this result is interesting on its own, it can also be applied within the formalism of Ref. [7] to define an improved *impact factor* for the gluon, which ensures that the description of $qg \rightarrow qg$ is exact (for 6 out of 8 helicity configurations, and for all 4 dominant ones). In Appendix B we present the improvements of the results in Ref. [7] on the description of jet production at the LHC, offered by the inclusion of these kinematically subleading corrections.

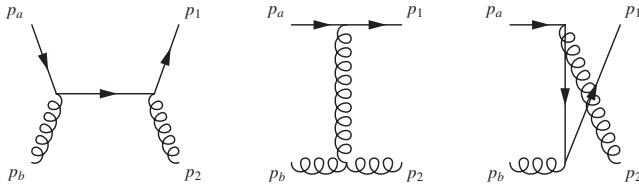


FIG. 1. The s -, t -, and u -channel processes which contribute to $q^-(p_a) + g^+(p_b) \rightarrow q^-(p_1) + g^+(p_2)$.

II. QUARK-GLUON SCATTERING

In this section we will evaluate the full, gauge-invariant, tree-level scattering amplitudes $\mathcal{M} = \mathcal{M}^{\rho\sigma} \varepsilon_\rho^*(p_2) \varepsilon_\sigma(p_b)$ for all 8 inequivalent helicity configurations in the scattering process $q(p_a) + g(p_b) \rightarrow q(p_1) + g(p_2)$. The aim is to display the close resemblance to the simpler case of qQ -scattering. In particular, we will see that for the helicity assignments, where a qQ -channel exists, the square of the qg -scattering matrix element is a factor depending only on the gluon momenta times the square of the simple qQ -scattering matrix element.

A. Helicity conserving amplitudes

We start with the helicity configuration $q^-(p_a) + g^+(p_b) \rightarrow q^-(p_1) + g^+(p_2)$. The simple relation to qQ -scattering is easily obtained with the following gauge choice for the polarization vectors:

$$\begin{aligned} \varepsilon_{2\sigma}^{+*} &= \frac{\bar{u}_b^- \gamma_\sigma u_2^-}{\sqrt{2} \bar{u}_b^- u_2^+} & \varepsilon_{2\sigma}^{-*} &= \frac{-\bar{u}_2^- \gamma_\sigma u_b^-}{\sqrt{2} \bar{u}_b^+ u_2^-} \\ \varepsilon_{b\rho}^+ &= \frac{-\bar{u}_2^+ \gamma_\rho u_b^+}{\sqrt{2} \bar{u}_2^+ u_b^-} & \varepsilon_{b\rho}^- &= \frac{\bar{u}_2^- \gamma_\rho u_b^-}{\sqrt{2} \bar{u}_2^- u_b^+}. \end{aligned} \quad (1)$$

This particular gauge choice gives a symmetric form, and keeps the factorization explicit between forward moving particles (p_a, p_1) and backward moving particles (p_b, p_2). Using the conventions outlined in Appendix A and the following shorthands:

$$\langle i|\mu|j \rangle = \bar{u}_i^- \gamma^\mu u_j^-, \quad \langle ij \rangle = \bar{u}_i^- u_j^+, \quad \text{and} \quad [ij] = \bar{u}_i^+ u_j^-, \quad (2)$$

we get (where A_x is the amplitude for the x -channel diagram in the chosen gauge)

$$\begin{aligned} A_s &= \frac{-ig^2 t_{ea}^b t_{1e}^2}{\hat{t}} \times \sqrt{\frac{p_{2\perp}^-}{p_b^-} \frac{p_{2\perp}^*}{|p_{2\perp}|}} \langle b|\sigma|2 \rangle \times \langle 1|\sigma|a \rangle. \\ A_t &= 0. \\ A_u &= \frac{-ig^2 t_{ea}^2 t_{1e}^b}{\hat{t}} \times \sqrt{\frac{p_b^-}{p_{2\perp}^-} \frac{p_{2\perp}^*}{|p_{2\perp}|}} \langle b|\rho|2 \rangle \times \langle 1|\rho|a \rangle. \end{aligned} \quad (3)$$

This gives the (obviously gauge-invariant) sum of

$$\begin{aligned} \mathcal{M} &= \frac{-ig^2}{\hat{t}} \times \frac{p_{2\perp}^*}{|p_{2\perp}|} \left(t_{ea}^b t_{1e}^2 \sqrt{\frac{p_b^-}{p_{2\perp}^-}} - t_{ea}^2 t_{1e}^b \sqrt{\frac{p_{2\perp}^-}{p_b^-}} \right) \\ &\quad \times \langle b|\sigma|2 \rangle \times \langle 1|\sigma|a \rangle. \end{aligned} \quad (4)$$

This is the full, tree-level amplitude for this helicity configuration. In the high energy limit ($p_b^- \sim p_{2\perp}^-$), the term in the brackets reduces to just a color matrix, and we find a contribution proportional to a t -channel pole and the contraction of two currents

$$\frac{g^2}{\hat{t}} f^{b2m} t_{1a}^m \times \frac{p_{2\perp}^*}{|p_{2\perp}|} \langle b|\sigma|2\rangle \times \langle 1|\sigma|a\rangle, \quad (5)$$

which agrees (up to an irrelevant phase and a color factor) with the structure for qQ -scattering. However, the crucial exact result in Eq. (4) is that this helicity amplitude for quark-gluon scattering is still expressible exactly as a scattering under exchange of a t -channel gluon current (despite the fact that the t -channel diagram itself is zero in this gauge). However, the current generated by the scattering of a gluon is slightly more complicated [by the terms in the brackets of Eq. (4)] than that generated by a quark. The color summed and averaged scattering matrix element is

$$|\mathcal{M}_{q^-g^+ \rightarrow q^-g^+}|^2 = \frac{g^4}{\hat{t}_{a1}\hat{t}_{b2}} \frac{C_F}{N_c^2 - 1} \left(\frac{1}{2} \frac{p_b^- + p_2^-}{p_b^- p_2^-} \left(C_A - \frac{1}{C_A} \right) + \frac{1}{C_A} \right) |\langle b|\rho|2\rangle \langle 1|\rho|a\rangle|^2. \quad (6)$$

In this case, $\hat{t}_{a1} = \hat{t}_{b2}$, but we write it this way in anticipation of the generalization to the multijet case. Cast in this form, we see directly that this helicity scattering of quarks and gluons is identical to that of the scattering of two different quark flavors with a replacement of C_F by the color factor

$$\frac{1}{2} \left(C_A - \frac{1}{C_A} \right) \left(\frac{p_b^-}{p_2^-} + \frac{p_2^-}{p_b^-} \right) + \frac{1}{C_A}. \quad (7)$$

We note that in the MRK limit ($p_b^- \rightarrow p_2^-$), this tends to C_A , as used in Ref. [7]. Equation (7) expresses how the strength of the coupling of the current increases with increasing acceleration of the scattering gluon [as $(\frac{p_b^-}{p_2^-} + \frac{p_2^-}{p_b^-})$ increases]. We will therefore call the result of Eq. (7) the *color acceleration multiplier* (CAM).

For the same process with positive helicity quarks ($q^+(p_a) + g^+(p_b) \rightarrow q^+(p_1) + g^+(p_2)$), the only difference is that $\langle 1|\rho|a\rangle$ becomes $\langle a|\rho|1\rangle$ which leads to the same gluon impact factor. The processes with negative helicity gluons can be found by taking the complex conjugate of these results, and because the new multiplicative factor is real, we again find the corresponding quark current multiplied by Eq. (7).

We see that the amplitudes for the assignments where the gluon helicity is *not* flipped all scale as \hat{s}/\hat{t} in the high energy limit—and the square of the scattering matrix element is given exactly by the corresponding qQ -case, multiplied by the same factor, depending only on the gluon momenta. All other helicity assignments are kinematically suppressed in the high energy limit.

The pure t -channel factorization in fact extends also to two-gluon scattering for the helicity configurations like $g^-(p_a)g^+(p_b) \rightarrow g^-(p_1)g^+(p_2)$, where the t -channel momentum is defined as $p_a - p_1 = -(p_b - p_2)$ (i.e. configurations where two unlike helicity gluons scatter into two

unlike helicity gluons). The full, gauge-invariant scattering amplitude can be put in the form

$$\mathcal{M}_{g^-g^+ \rightarrow g^-g^+} = \frac{-ig^2}{t} \langle 1|\mu|a\rangle \langle b|\mu|2\rangle \frac{p_{2\perp}^*}{|p_{2\perp}|} \sqrt{\frac{p_1^+}{p_a^+}} \times \left(f^{amb} f^{m12} \sqrt{\frac{p_2^-}{p_b^-}} + f^{a2m} f^{m1b} \sqrt{\frac{p_b^-}{p_2^-}} \right). \quad (8)$$

This once again has the current structure of the simple $qQ \rightarrow qQ$ amplitude, multiplied by similar factors as found in Eq. (4).

B. Helicity-flipping amplitudes

Returning to $qg \rightarrow qg$ -scattering, the cases where the gluon flips helicity are more complicated, but can be cast in a very similar form. The two distinct cases are $q^-g^- \rightarrow q^-g^+$, which gives

$$\begin{aligned} A_s &= \frac{ig^2 t_{ea}^b t_{1e}^2}{\hat{t}} \times \left(\sqrt{\frac{p_2^-}{p_b^-}} \frac{p_{2\perp}}{|p_{2\perp}|} \langle b|\sigma|2\rangle + 2p_b^\sigma \frac{\hat{t}}{\hat{s}} \right) \times \langle 1|\sigma|a\rangle \\ A_t &= -g^2 t_{1a}^m f^{m2b} \times \frac{(p_2 + p_b)^\mu}{\hat{t}} \times \langle 1|\mu|a\rangle \\ A_u &= \frac{-ig^2 t_{ea}^2 t_{1e}^b}{\hat{t}} \times \left(\sqrt{\frac{p_b^-}{p_2^-}} \frac{p_{2\perp}^*}{|p_{2\perp}|} \langle 2|\rho|b\rangle + 2p_2^\rho \frac{\hat{t}}{\hat{u}} \right) \times \langle 1|\rho|a\rangle, \end{aligned} \quad (9)$$

and $q^-g^+ \rightarrow q^-g^-$ which gives

$$\begin{aligned} A_s &= \frac{ig^2 t_{ea}^b t_{1e}^2}{\hat{t}} \times \sqrt{\frac{p_2^-}{p_b^-}} \frac{p_{2\perp}^*}{|p_{2\perp}|} \langle 2|\sigma|b\rangle \times \langle 1|\sigma|a\rangle \\ A_t &= -g^2 t_{1a}^m f^{m2b} \times \frac{(p_2 + p_b)^\mu}{\hat{t}} \times \langle 1|\mu|a\rangle \\ A_u &= \frac{-ig^2 t_{ea}^2 t_{1e}^b}{\hat{t}} \times \sqrt{\frac{p_b^-}{p_2^-}} \frac{p_{2\perp}}{|p_{2\perp}|} \langle b|\rho|2\rangle \times \langle 1|\rho|a\rangle. \end{aligned} \quad (10)$$

We see that only for the helicity configuration where the incoming gluon has the same helicity as that of the quark *and* the helicity of the gluon is flipped is there a contribution which is *not* expressible as a simple current contraction over a t -channel pole. Only these two (kinematically suppressed) helicity configurations give rise to the poles in the \hat{u} - and \hat{s} -channel.

In the current study, we focus on the t -channel pole, and will therefore neglect the additional terms in Eq. (10), which are suppressed in the MRK limit as $\hat{s}/\hat{t} \rightarrow \infty$, $\hat{s} \rightarrow -\hat{u}$. The description of the t -channel pole is obviously still gauge-invariant.

The amplitudes with positive helicity quarks can be obtained by complex conjugation. We notice that between Eqs. (9) and (10), A_s and A_u are swapped (as we would expect). One can check explicitly that the amplitudes where the gluon changes helicity all vanish in the MRK limit. This should be compared with the scaling as \hat{s}/\hat{t} in

the MRK limit for the helicity amplitudes studied in Sec. II A.

We now seek to find the equivalent of Eq. (6) for the nonhelicity conserving amplitudes. We use the shorthands

$$j_{ij}^{-,\mu} = \langle j|\mu|i\rangle, \quad \text{and} \quad j_{ij}^{+,\mu} = \langle i|\mu|j\rangle. \quad (11)$$

$$\begin{aligned} |M_{q^-g^+ \rightarrow q^-g^+}^t|^2 &= \frac{g^4}{\hat{t}_{a1}\hat{t}_{b2}} \frac{1}{C_A(N_C^2 - 1)} \frac{C_F}{2} * \left((C_A^2 - 1) \left(\frac{p_2^-}{p_b^-} |j_{b2^+}^+ j_{a1^-}^-|^2 + \frac{p_b^-}{p_2^-} |j_{b2^-}^- j_{a1^-}^-|^2 \right) \right) + 2C_A^2 |(p_2 + p_b) \cdot j_{a1^-}^-|^2 \\ &+ 2C_A^2 \sqrt{\frac{p_2^-}{p_b^-}} \Re \left[\frac{p_{2\perp}^*}{|p_{2\perp}|} \cdot (p_2 + p_b) \cdot j_{a1^-}^- \cdot (j_{b2^+}^+ j_{a1^-}^-)^* \right] + 2C_A^2 \sqrt{\frac{p_b^-}{p_2^-}} \Re \left[\frac{p_{2\perp}}{|p_{2\perp}|} \cdot (p_2 + p_b) \cdot j_{a1^-}^- \cdot (j_{b2^-}^- j_{a1^-}^-)^* \right] \\ &+ 2\Re \left[\frac{p_{2\perp}}{|p_{2\perp}^*|} j_{b2^+}^+ j_{a1^-}^- \cdot (j_{b2^-}^- j_{a1^-}^-)^* \right]. \end{aligned} \quad (12)$$

The result for $|M_{q^-g^+ \rightarrow q^-g^+}^t|^2$ (in this case equal to $|\mathcal{M}_{q^-g^+ \rightarrow q^-g^+}^t|^2$) is very similar, with the j_{b2} currents reversed and appropriate phases complex conjugated, as can be seen by comparing Eqs. (9) and (10). While these matrix elements are more complicated than Eq. (4), they are just the sum of terms of contractions of currents for specific helicity configurations, plus a new one $(p_2 + p_b)$ which is necessary for the description of the spin-flip of the gluon.

We note in passing that in all the results discussed so far, the gluon has been taken to be moving in the backward direction. This is obviously an arbitrary choice, but the choice of light-cone directions results in a complex phase arising from the conventions for the spinors, given in Appendix A.

The overall conclusion of this section is that using scattering of helicity states, it is possible to extract a gauge-invariant definition of the t -channel pole generated by the deflection of a gluon. Only two out of eight non-equivalent helicity configurations have a contribution which cannot be ascribed to a pure t -channel pole (and these helicity configurations are suppressed in the MRK limit).

In Appendix B we show some sample results of including this new approach to gluon channels in the formalism of Ref. [7].

III. CONCLUSIONS

By exploring the scattering of specific helicity states in quark-gluon scattering at tree-level we have shown explicitly that the t -channel pole can be described exactly as a contraction of two local currents. Furthermore, we demonstrate that out of eight nonzero helicity configurations, only two suppressed possibilities have contributions that are not pure t -channel poles. We extract a gauge-invariant definition for the t -channel current generated by the scattering of a gluon.

This at the same time directly proves the assertions on the generality of quark and gluon scattering in the multi-

Then the matrix element squared with summed and averaged color is (M^t denotes the t -channel factorized approximation to the full \mathcal{M})

Regge kinematic (MRK) limit made in Ref. [7], and offers slight improvements in the description of scattering amplitudes in the subasymptotic region. The formalism developed here is immediately applicable in the resummation program developed on the basis of Ref. [7] for the description of production of pure multijets, and multiple jets in association with a W , Z , or H -boson.

ACKNOWLEDGMENTS

J. M. S. would like to thank the CERN theory group for kind hospitality and is supported by the UK Science and Technology Facilities Council (STFC). This work was supported by the E. C. Marie-Curie Research Training Network ‘‘Tools and Precision Calculations for Physics Discoveries at Colliders’’ under Contract No. MRTN-CT-2006-035505.

APPENDIX A: SPINOR REPRESENTATION

We use the following representation for the spinors. For outgoing particles with 4-momentum p , $p^\pm = E \pm p_z$, and $p_\perp = p_x + ip_y$, we use

$$u^+(p) = \begin{pmatrix} \sqrt{p^+} \\ \sqrt{p^-} \frac{p_\perp}{|p_\perp|} \\ 0 \\ 0 \end{pmatrix} \quad \text{and} \quad u^-(p) = \begin{pmatrix} 0 \\ 0 \\ \sqrt{p^-} \frac{p_\perp^*}{|p_\perp|} \\ -\sqrt{p^+} \end{pmatrix}. \quad (A1)$$

For incoming particles with 4-momentum p moving in the $+$ direction, we use

$$u^+(p) = \begin{pmatrix} \sqrt{p^+} \\ 0 \\ 0 \\ 0 \end{pmatrix} \quad \text{and} \quad u^-(p) = \begin{pmatrix} 0 \\ 0 \\ 0 \\ -\sqrt{p^+} \end{pmatrix}. \quad (A2)$$

For incoming particles with 4-momentum p moving in the $-$ direction, we use

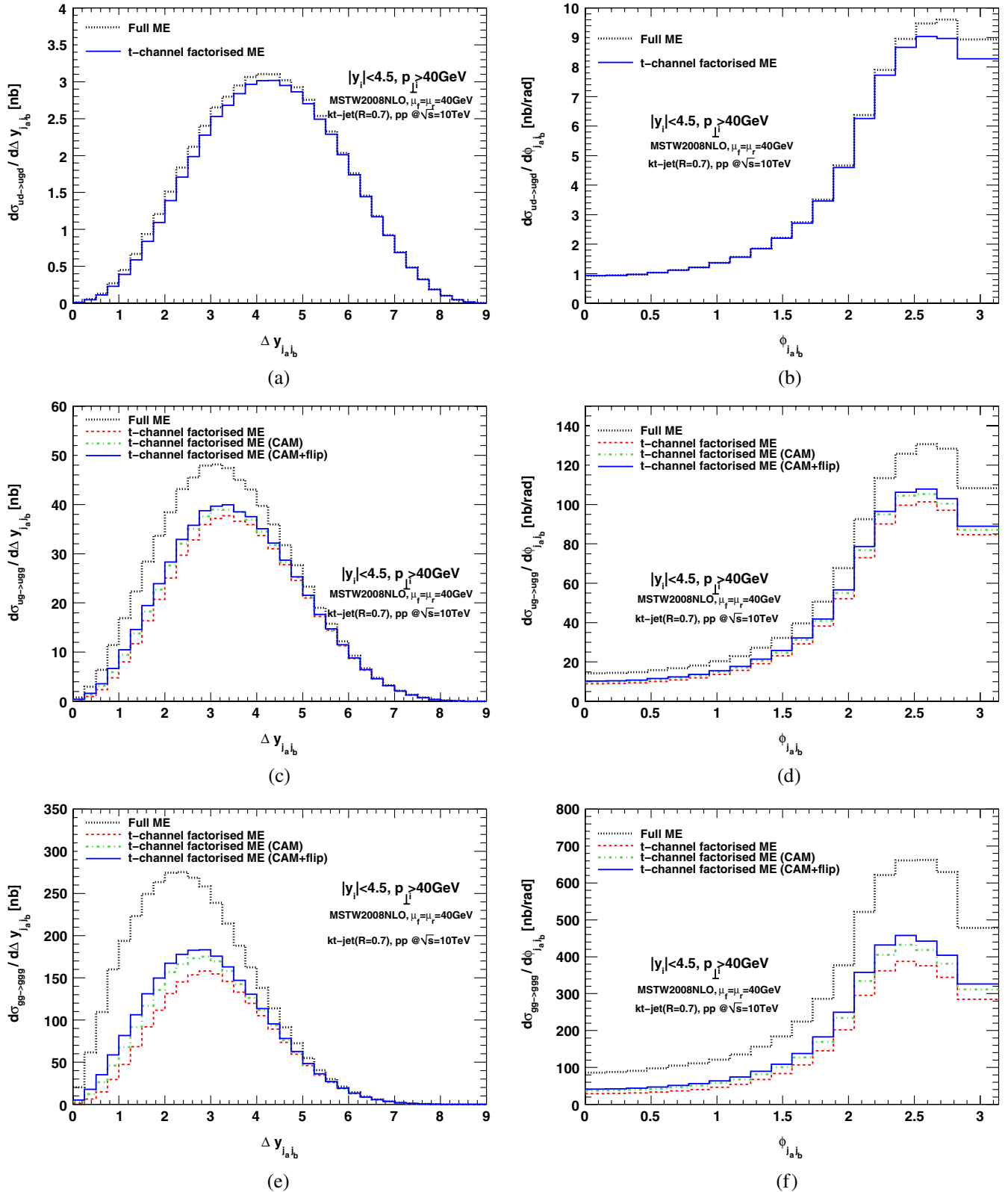


FIG. 2 (color online). Results for $d\sigma/d\Delta y$ and $d\sigma/d\phi$ for $ud \rightarrow ugd$ (a) and (b), $ug \rightarrow ugg$ (c) and (d), and $gg \rightarrow ggg$ (e) and (f). Δy is the rapidity difference between the most forward and most backward hard jet. The black dashed line represents the full matrix element, the red dashed line is the implementation based on the scattering of quark currents [7], the full blue line is this result with the color adjusted multiplier (CAM) of Eq. (7) and the green dashed line has the CAM and the effect of flipped helicities, Eq. (12).

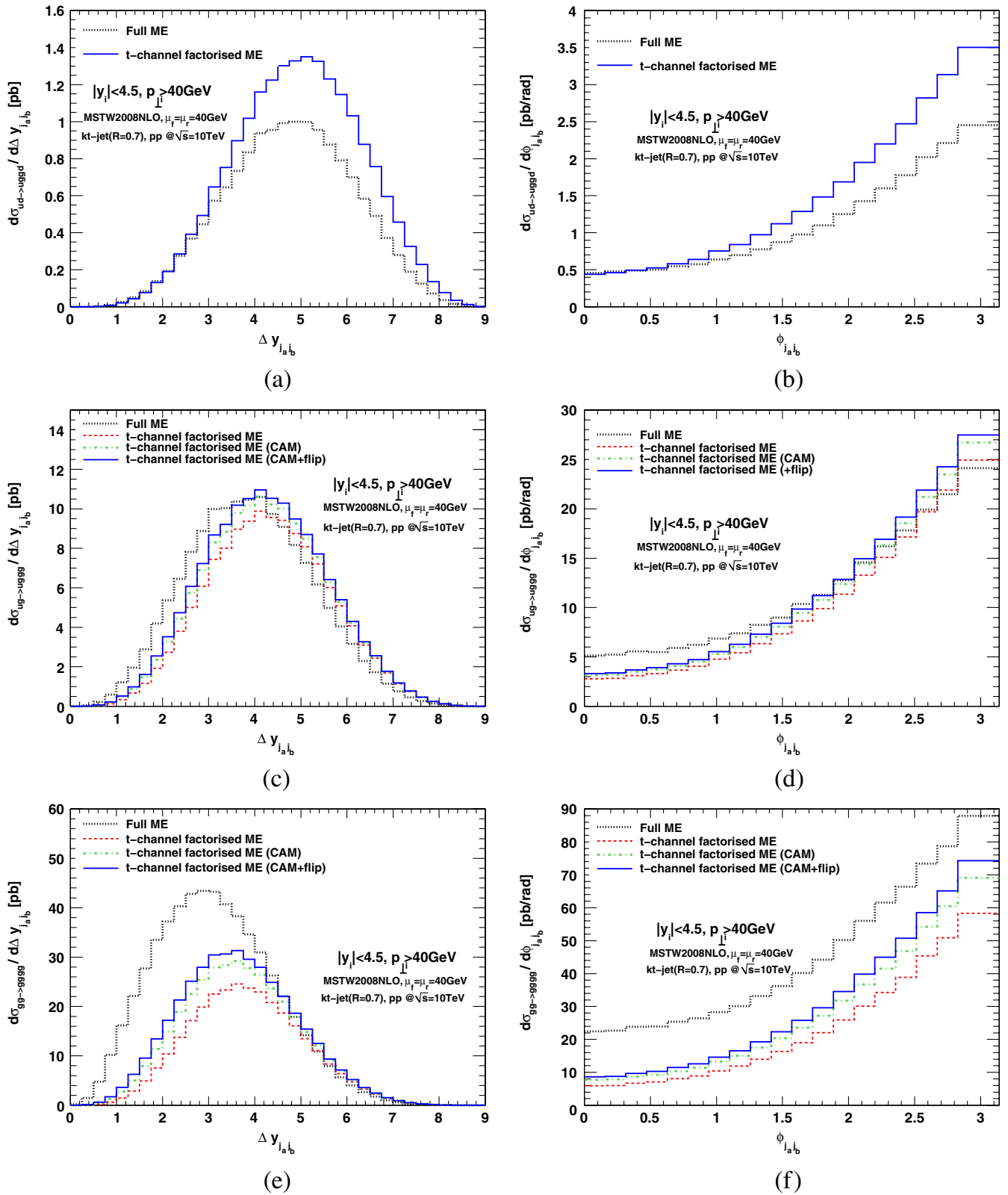


FIG. 3 (color online). As in Fig. 2, but now for the 4 jet final states: $ud \rightarrow uggd$ (a) and (b), $ug \rightarrow uggg$ (c) and (d), and $gg \rightarrow gggg$ (e) and (f).

$$u^+(p) = \begin{pmatrix} 0 \\ -\sqrt{p^-} \\ 0 \\ 0 \end{pmatrix} \quad \text{and} \quad u^-(p) = \begin{pmatrix} 0 \\ 0 \\ -\sqrt{p^-} \\ 0 \end{pmatrix}. \quad (\text{A3})$$

We use the following representation for the gamma matrices:

$$\begin{aligned} \gamma^0 &= \begin{pmatrix} 0 & 0 & 1 & 0 \\ 0 & 0 & 0 & 1 \\ 1 & 0 & 0 & 0 \\ 0 & 1 & 0 & 0 \end{pmatrix}, & \gamma^1 &= \begin{pmatrix} 0 & 0 & 0 & -1 \\ 0 & 0 & -1 & 0 \\ 0 & 1 & 0 & 0 \\ 1 & 0 & 0 & 0 \end{pmatrix}, \\ \gamma^2 &= \begin{pmatrix} 0 & 0 & 0 & i \\ 0 & 0 & -i & 0 \\ 0 & -i & 0 & 0 \\ i & 0 & 0 & 0 \end{pmatrix}, & \gamma^3 &= \begin{pmatrix} 0 & 0 & -1 & 0 \\ 0 & 0 & 0 & 1 \\ 1 & 0 & 0 & 0 \\ 0 & -1 & 0 & 0 \end{pmatrix}. \end{aligned} \quad (\text{A4})$$

APPENDIX B: RESULTS

Here, we show comparisons between the full matrix element, obtained from MADGRAPH 11, and the results obtained in the t -channel factorized picture of Ref. [7]. We will concentrate on the changes introduced by this current study compared to the description in Ref. [7], and will not show the results for just 2-jet rates, since here the approximations are so good that the difference to the full tree-level result is completely insignificant.

Within the t -channel factorized approximation, the case of $2 \rightarrow 2$ helicity-nonflipping pure gluon scattering ($gg \rightarrow gg$) is described as simply the scattering of two quark-generated currents, but with a color acceleration multiplier [Eq. (7)] for each current. The possibility of one helicity-flipping is then described simply as Eq. (12), but with an extra CAM for the nonflipping gluon current. Since the contribution from the single gluon helicity-flipping amplitudes is small, we refrain from a description of the (double

suppressed) contribution of a flip in the helicity of both scattered gluons.

The square of the $2 \rightarrow n$ -scattering amplitude is approximated by the sum over the square of the basic $2 \rightarrow 2$ current contractions (for each helicity possibility), multiplied by one (gauge-invariant) effective vertex for each additional gluon emission. See Ref. [7] for further details.

Figures 2 and 3 show the results for 3- and 4-jet final states respectively (for both qg and gg initiated processes) within the following cuts (identical to the ones used in Ref. [7]):

$$p_{j\perp} > 40 \text{ GeV} \quad |y_j| < 4.5.$$

We show the differential cross section with respect to Δy , the rapidity difference between the two jets extremal in rapidity, and ϕ , the angle in the transverse plane between these outer jets. These are just examples to illustrate the accuracy obtained in the perturbative approximations. There is obviously no change compared to Ref. [7] in the cases of quark-quark-initiated processes, which are just included here for completeness.

One can see that the effect of multiplying by the adjusted color factor, Eq. (7), alone (green lines, marked CAM in Figs. 2 and 3) gives an improvement in all cases. It has a greater effect in the 4-jet cases compared to 3-jet cases, which agrees with the interpretation of it as a contribution from the acceleration of the gluon. One would expect this to be greater when an extra jet is produced, and we do indeed see a greater effect. We then see a further, more modest, improvement when the channels where the helicity of one of the gluons changes are also incorporated through Eq. (12). The blue solid line in the plots is the sum total of improvements, and is obtained within a formalism which, according to the results of Ref. [7], is sufficiently simple that all orders in the perturbative series can be summed directly. We did not go to higher than 4-jet final states here because of the time it would take for the full matrix element results. We were not limited by the time for our formalism; the 4-jet results took about 5 minutes on a single computer.

-
- [1] M. Bahr *et al.*, *Eur. Phys. J. C* **58**, 639 (2008).
 [2] T. Sjostrand, S. Mrenna, and P. Skands, *Comput. Phys. Commun.* **178**, 852 (2008).
 [3] T. Gleisberg *et al.*, *J. High Energy Phys.* **02** (2009) 007.
 [4] V. S. Fadin, E. A. Kuraev, and L. N. Lipatov, *Phys. Lett.* **60B**, 50 (1975).
 [5] E. A. Kuraev, L. N. Lipatov, and V. S. Fadin, *Zh. Eksp. Teor. Fiz.* **71**, 840 (1976) [*Sov. Phys. JETP* **44**, 443 (1976)].
 [6] E. A. Kuraev, L. N. Lipatov, and V. S. Fadin, *Zh. Eksp. Teor. Fiz.* **72**, 377 (1977) [*Sov. Phys. JETP* **45**, 199 (1977)].
 [7] J. R. Andersen and J. M. Smillie, *J. High Energy Phys.* **01** (2010) 39.
 [8] J. R. Andersen and C. D. White, *Phys. Rev. D* **78**, 051501 (2008).
 [9] J. R. Andersen, V. Del Duca, and C. D. White, *J. High Energy Phys.* **02** (2009) 015.
 [10] B. L. Combridge and C. J. Maxwell, *Nucl. Phys.* **B239**, 429 (1984).